White Rose Research Online

eprints@whiterose.ac.uk
https://eprints.whiterose.ac.uk
Universities of Leeds, Sheffield and York

Deposited via The University of Leeds.

White Rose Research Online URL for this paper:
https://eprints.whiterose.ac.uk/id/eprint/228140/

Version: Accepted Version

Article:
Atkinson, J.W., Wignall, P.B. and Page, K.N. (2020) The Hettangian–Sinemurian (Lower Jurassic) strata of Redcar, Cleveland Basin, NE England: facies and palaeoecology. Proceedings of the Yorkshire Geological Society, 63 (2). pp. 77-87. ISSN: 0044-0604

https://doi.org/10.1144/pygs2019-011

© 2020 The Author(s). This is an author produced version of an article published in Proceedings of the Yorkshire Geological Society (PYGS). Uploaded in accordance with the publisher's self-archiving policy.

Reuse
Items deposited in White Rose Research Online are protected by copyright, with all rights reserved unless indicated otherwise. They may be downloaded and/or printed for private study, or other acts as permitted by national copyright laws. The publisher or other rights holders may allow further reproduction and re-use of the full text version. This is indicated by the licence information on the White Rose Research Online record for the item.

Takedown
If you consider content in White Rose Research Online to be in breach of UK law, please notify us by emailing eprints@whiterose.ac.uk including the URL of the record and the reason for the withdrawal request.

The Hettangian-Sinemurian (Lower Jurassic) strata of Redcar, Cleveland Basin, NE England: facies and palaeoecology

J.W. Atkinson[1]*, P.B. Wignall[1] & K.N. Page[2]

[1]School of Earth and Environment, University of Leeds, Leeds. LS2 9JT, UK

*gy12jwa@leeds.ac.uk

[2]Camborne School of Mines, University of Exeter, Penryn Campus, Penryn, Cornwall TR10 9FE, UK

Abstract

The foreshore at Redcar hosts the oldest Jurassic succession exposed on the Yorkshire-Cleveland Coast but has received little attention since the late 19th century. Temporary removal of beach sands by winter storms early in 2018 allowed for a sedimentological and palaeontological study of a nearly 60 m-thick foreshore section. The rocks are latest Hettangian to early Sinemurian in age (Early Jurassic) and comprise five coarsening-upward cycles (parasequences) that grade from mudstones through siltstones into *Gryphaea*-rich shell beds. Ammonites are reasonably common along with a diverse benthos that includes abundant bivalves (e.g. *Gryphaea, Cardinia, Luciniola, Plagiostoma* and *Oxytoma*) and rarer serpulids, gastropods, foraminifera and solitary corals. In the upper part of the section thicker-shelled taxa are commonly bored by cirripedes and bryozoans. Despite relatively high benthic diversity and intense bioturbation, pyrite framboids are common with size distributions suggesting deposition under a moderately oxygen-restricted water column. The Redcar succession postdates the end-Triassic mass extinction by as much as 4 million

years and the diverse marine assemblages indicate recovery was substantially complete by this time.

Keywords: pyrite framboid, marine recovery, dysoxia, *Gryphaea*

Introduction

The Cleveland Basin, North Yorkshire and Cleveland, preserves one of the classic Lower Jurassic successions that has provided important evidence on numerous aspects of the Early Jurassic world, such as the Toarcian Oceanic Anoxic Event (e.g. Little & Benton 1995; McArthur *et al.* 2000; Cohen *et al.* 2004; Kemp *et al.* 2005; Wignall *et al.* 2005; Danise *et al.* 2013) and the Global Stratotype Section and Point (GSSP) for the Sinemurian-Pliensbachian stage boundary (Meister *et al.* 2004). Earlier stratigraphic intervals in the Lower Jurassic have been relatively neglected because of poor coastal exposures and scarcity of inland records, which mostly comprise temporary exposures recorded in the 19th century (Tate & Blake 1876), or borehole studies (Ivimey-Cook & Powell 1991; Powell *et al.* 1992). Redcar Rocks is the only locality in the Cleveland Basin where rocks of the Hettangian and lowermost Sinemurian are currently exposed. The intertidal platforms were meticulously sampled by Tate and Blake and their results were published in 1876. Their bed descriptions are somewhat difficult to interpret but they provided a useful sketch map of the foreshore depicting the locations of key ammonite finds (expanded in Page 2004a). The succession was subsequently reported in Gad's (1966) unpublished PhD thesis and by van Buchem & McCave (1989) although neither provided a detailed section nor any palaeontological study. Lord (1971) published a taxonomic study of the ostracods of the Redcar section and remarked that 'it is hoped that a full revision of this fine section

will not be long delayed' (Lord, 1971, p.644). The problem with the Redcar succession is its frequent cover beneath beach sand, as Tate & Blake (1876, p. 56) noted: - 'the occasions, however, when so large an expanse of rock is in view, as we have shown on the plan, are few'. Fortunately, the storms in February-March 2018 removed great quantities of the sand cover exposing a section almost as good as seen by Tate & Blake more than 140 years before. Our study provides a detailed log of the sedimentary succession alongside a record of fossil occurrences. We assess the palaeoenvironments through analysis of fossil communities, sedimentary facies and reconstruction of palaeo-redox conditions using framboidal pyrite size distributions (cf. Atkinson & Wignall 2019). Redcar Rocks provide a new perspective on the Hettangian and Sinemurian interval that allows comparison with the East Midlands Shelf and the well-documented Blue Lias Formation of southwest Britain and contributes new data on the changing environmental conditions and biotic recovery following the end-Triassic mass extinction event.

Geological setting

The Cleveland Basin formed as part of a series of small extensional basins within a shallow epicontinental seaway (Powell 2010). During the Early Jurassic the basin was bordered by the Pennine High landmass to the west and the Market Weighton High to the south (e.g. Powell 2010, Fig. 2). The oldest Jurassic-aged rocks within the Cleveland Basin are assigned to the Redcar Mudstone Formation, a mudstone- and siltstone-rich succession that is divided into the following members: a lowermost Calcareous Shale Member defined by the presence of carbonate nodules; the Siliceous Shale Member, bearing sandy horizons; the Pyritous Shale Member, a dark shale rich in pyrite, and the Ironstone Shale Member, characterized by beds of

siderite nodules (Fig. 1). The Redcar Mudstone Formation is between 250 and 283 m thick near Redcar, thinning southwards (Powell 1984). The Redcar Rocks outcrop exposes much of the Calcareous Shale Member, while the nearby Coatham Rocks reveal higher strata in the Redcar Mudstone Formation and the overlying Pliensbachian-aged Staithes Sandstone Formation, albeit only at very low tide (Figs. 1 & 2). Exposure is discontinuous, and some intervals remain obscured even when much of the beach sand has been removed. In the cliffs and foreshore exposures of Robin Hood's Bay some 40 km to the southeast, only the upper *c.* 20 m of the Calcareous Shale are exposed, meaning that these lower beds can be studied only at Redcar (Fig. 1).

Materials and methods

Logging of the Calcareous Shale Member was undertaken along the foreshore at Redcar Rocks using a high-precision Jacob's staff with laser sight (Patacci 2016), and sampled beds were allocated numbers, Red 1 – 31 (non-sequentially, omitting Red 25). Benthic diversity was assessed by species counts at semi-regular intervals. Fossils within rock masses were identified on freshly split surfaces of approximately equal volume of mudstone (~0.5 x 0.5 x 0.3 m). In exposed shell beds, fossils were identified *in situ* on bedding surfaces. Species range extensions are inferred from occurrences higher in the succession at Robin Hood's Bay, Staithes and Hawsker Bottoms based on data presented in Atkinson and Wignall (2020). To reduce the effects of sampling intensity and smooth the resulting diversity curve, Range Through (RT) species richness was calculated – this is the sum of observed, raw species counts and ghost ranges per sample horizon. Sediments were also studied in thin sections

which allowed occurrences of microfossils (especially foraminifera) and shell fragments to be noted.

A subset of the sampled horizons was analysed for changes in oxygenation regime using pyrite framboids. Framboids are spheres of aggregated pyrite microcrysts that form at the boundary between oxic and sulphidic waters (Wilkin *et al.* 1996). Under euxinic conditions (free H_2S) the redox boundary occurs in the water column and framboids grow to around 5 µm in diameter before they sink down from the chemocline and cease to grow. Pyrite framboid populations from such settings have a small mean diameter and show a narrow size range (Wilkin *et al.* 1996). In oxic-dysoxic settings the redox boundary is within the uppermost sediments allowing framboids to grow to larger and more varied sizes as they can remain at the chemocline for longer (Wilkin *et al.* 1996). Although Wilkin *et al*. (1996) suggested it was not possible to distinguish framboids that formed in the sediment under a dysoxic water column from those that formed in the sediment under an oxic water column, the former conditions are generally characterised by much greater numbers of framboids (Wignall & Newton 1998). Employing the method from Wignall & Newton (1998), pyrite framboid diameters were measured from carbon-coated polished stone chips approximately 2 x 1 cm in size set into resin blocks, and viewed using a Tescan VEGA3 XM Scanning Electron Microscope (SEM) with a backscatter electron detector. Ideally 100 framboids were measured from each sample within a designated one-hour analysis time. Mean framboid diameter and standard deviation were calculated for each sample and plotted on what is referred to herein as a Wilkin diagram (cf. Wilkin *et al.* 1996).

Results

Sedimentology

The measured section spans a thickness of some 50 metres predominantly of mudstone and silty mudstone with thin, calcareous, shell-rich beds (Fig. 3). Spacing of shell beds occurs with some degree of cyclicity. This can be seen on a foreshore map, where closely spaced shell beds form resistant scars, or intertidal headlands, with less resistant mudstones containing fewer shell beds forming the embayments in-between (Fig. 2). Between 16-22 m from the base of the measured section (beds 66-98 of Tate & Blake 1876) there are 16 closely spaced shell beds forming the intertidal headland known as Jenny Leigh's Scar (Fig. 2). Shell beds between 36-38 m form another intertidal headland, Stokesley Scar (beds 35-53 of Tate & Blake). Above 42 m, shell beds and sandy intercalations become proportionally more dominant, forming East Scar (beds 32-11 of Tate & Blake).

The mudstones are medium to light grey in colour with little of the primary fabric retained owing to pervasive bioturbation, resulting in silt-grade quartz and detrital carbonate grains being scattered throughout and shell fragments often rotated to high angles (Fig. 4A). Sporadic horizons of carbonate concretions occur within the mudstone intervals usually in close association with shell beds. Between around 24-32 m (beds 55-64 of Tate & Blake) siderite nodules are found either scattered or forming distinct horizons, with this part of the succession having the lowest concentration of shell beds (Fig. 3).

Individual shell beds are up to 0.3 m thick and include large numbers of disarticulated *Gryphaea* and *Cardinia* shells (Figs. 4B & 5) with abundant thinner shelled debris, including recognisable bivalve and echinoderm fragments. The lower parts of the shell beds consist of mudstone with a high proportion of thin shell fragments, grading up into siltier and sandier strata with larger and more numerous bioclasts, mostly *Gryphaea,* culminating in shelly limestones cemented by sparite (i.e.

biosparite, Fig. 4C). Small lenses of mudstone can persist between larger shells in these biosparites. Shell beds sampled at horizons Red 8, 9, 15 and 17 all contain glauconite-replaced echinoderm fragments.

Above 40 m the succession becomes increasingly silty, until at 42-47 m where fine sandstones form East Scar (Figs. 2 & 3). Each bed is composed of homogeneous siltstone with quartz and detrital carbonate grains, grading up into carbonate-cemented fine-grained sandstone rich in shell debris and *Gryphaea*. This part of the succession also features elongate, cigar-shaped phosphatic nodules, approximately 5 cm long, which preserve burrow mottling (Fig. 4D).

Viewed under a SEM, many of the Redcar beds feature diagenetic ankerite grains, ovoid in shape and typically <10 µm in length, often at high abundances within some samples (Fig. 6A). Thin sections show that iron oxide is common in Red 27 and 29, both as discrete grains and infills of foraminifera tests, which may originally have been siderite or pyrite grains and pyrite infills respectively, prior to oxidation.

Fauna

Ammonite faunas collected from the lower 9 m of the section are dominated by *Schlotheimia* of the Angulata Chronozone, of latest Hettangian age (Fig. 7A). These are replaced by Arietitidae in the basal Sinemurian, Conybeari Subchronozone (Bucklandi Chronozone), including *Metophioceras* spp.. Unfortunately, no ammonites were found from Jenny Leigh's Scar during this survey, although previously reported finds include *Coroniceras* ex grp *rotiforme* (J. de C. Sowerby) indicating the Rotiforme Subchronozone is present on the scar (Page 2004a).

Placement of the Rotiforme-Bucklandi Subchronozone boundary is still unclear, although *Coroniceras* ex grp *multicostatum* (J. Sowerby) was collected from Red 14 suggesting the late Bucklandi Subchronozone is present (multicostatum Biohorizon Sn14 of Page 1992, 2010). The lowest part of the succeeding Semicostatum Chronozone is recognisable by occurrences of *Paracoroniceras* sp. in the upper beds of Stokesley Scar, with well-preserved and, occasionally, encrusted examples of *Arnioceras* collected from the mudstones above (Fig. 7B). The Scipionanum Subchronozone is recognised by *Agassiceras* with *Arnioceras acuticarinatum* (Simpson) collected from Red 29 and Red 30.

Based upon range through (RT) species richness, total benthic diversity was modest during the Angulata Chronozone with fewer than 10 species present, but then rises markedly to 15 species in the first shell bed of Jenny Leigh's Scar. Above this level benthic diversity increases further to around 22 species and remains stable for the remainder of the succession (Fig. 8). The assemblages are dominated by bivalves with a broad range of ecologies present. Of the suspension feeding guilds of bivalve there is one epifaunal reclining species, three cementing, one epifaunal facultative motile, eight epibyssate and three endobyssate, four shallow infaunal, including one abundant species that likely hosted sulphur-oxidising chemosymbiotic bacteria, and also two deep infaunal taxa (Table 1). Deposit-feeding bivalves were also common with six species recorded. After bivalves, gastropods form the next significant component with large forms present (up to 66 mm height and width) such as *Pleurotomaria cognata* Chapuis & Dewalque (Fig. 7C), although most are small (~1-2 mm) high-spired forms seen only in thin section (Fig. 7D). Echinoderms, especially echinoid spines and ophiuroid plates, are a common component of the shell beds. Red 12 also contains articulated specimens of *Isocrinus psilonoti* (Quenstedt) including cirri

(Fig, 7E). Serpulids are locally common and several species are present, with dense, intergrown nests of small diameter specimens found in Red 8 (Fig. 4E).

Gryphaea arcuata Lamarck occurs throughout the entire succession and is the most conspicuous fossil, especially in the shell beds where their thick shells dominate (Fig. 5). In the upper shell beds of Jenny Leigh's Scar, the thick-shelled *Cardinia listeri* (J. Sowerby) is also found in high numbers alongside *G. arcuata*. Shell beds also contain subordinate faunas including *Luciniola limbata* (Terquem & Piette) and the solitary coral *Trocharea guettardi* (Blaniville) (c. 35 m, bed 55 of Tate & Blake). *Cardinia* and *Gryphaea* specimens in the shell beds of Stokesley and East Scar frequently display a range of borings, which are infilled by matrix testifying they are of Jurassic origin (Fig. 7F-L). Most are slit-like in form and pinched at one end, typical of barnacle borings (Häntzschel 1975) such as *Zapfella, Rogerella* and *Simonizapfes;* the last has a distinctive sock-shaped cross section, seen in a broken *Cardinia* from Red 15 (Fig. 7J). A fine network-like boring was seen on *Cardinia* shells. These do not penetrate the shell to any significant depth however, and may have been formed by boring bryozoans (Fig. 7K). Other borings include simple rounded holes and elongate gashes (Fig. 7H). Evidence for constrained growth in a specimen of *Cardinia* was also found. This specimen shows that normal growth was impeded partway through the individual's life resulting in irregular growth lines and a miss-shaped outline, and may indicate overcrowding (Fig. 7L).

Borings are very rare in the shell beds of Jenny Leigh's Scar and shells are generally in a better state of preservation, with articulated *Cardinia* notably more common.

Although fossils are most conspicuous in the shell beds many species occur within the mudstones, including thin-shelled protobranch species, *Luciniola limbata,*

Oxytoma inequivalvis (J. Sowerby) and *Pseudolimea pectinoides* (J. Sowerby) (Fig. 8). Large logs of fossilised wood were also noted.

Tate & Blake (1876) reported four coral-hosting beds at Redcar, but only their second uppermost coral bed (Red 16 = bed 55 of Tate & Blake) was seen during this study, which hosts solitary coral *Trocharea guettardi* (Blainville) and scallop *Chlamys textoria* (Schlotheim). Solitary corals like *Trocharea* are widespread in the Angulata and Bucklandi chronozones of the British Isles (Negus 1983), being recorded from Lincolnshire (Brandon *et al.* 1990), Larne in Northern Ireland (Negus 1983) and Glamorgan, South Wales (Trueman 1930).

Foraminifera were identified from thin sections and are predominately elongate, uniserial taxa (*Pseudonodosaria*, *Paralingula*, *Dentalina*), that occupy a shallow infaunal niche (Rita *et al.* 2016). *Glomospirella*, an epifaunal form with discoidal coiled morphology (Rita *et al.* 2016) was found in Red 2. Red 27 hosted the greatest abundance of foraminifera with numerous examples of *Lenticulina,* an opportunistic taxon. Ostracods were also encountered in several beds (Red 2, 3, 15, 20, 24).

Framboidal pyrite analysis

Pyrite was found in all samples, both as euhedral crystals and framboidal pyrite, and locally forming a pyrite cement (Red 28). Framboids often occur in clusters or streamers surrounded by clouds of dissociated pyrite microcrysts (Fig. 6B). During the one-hour per sample analysis time over 100 framboids were counted from each polished chip, save for two samples which contained >70 framboids each. All samples show framboid populations that plot in the middle to upper oxic-dysoxic field of the Wilkin diagram (Figs. 3 & 9). There is no distinction between framboid populations

measured from shell beds and mudstones, and equally no systematic change in average framboid diameters or standard deviation up-section. Overall, the measured succession contains framboids with average diameter of 8.35 μm and standard deviation of 4.31 μm.

Discussion

Redcar presents a mudstone-dominated succession encompassing the Hettangian-Sinemurian (Angulata-Bucklandi chronozones) boundary, with a reasonably diverse benthic fauna. Five distinct parasequences (shallowing-up cycles) are recognised, each passing upwards from mudstone-dominated to shell bed-dominated facies. The associated grain size increase suggests the shelly horizons represent shallower/more proximal environments. The first parasequence forms the base of the exposed section to the top of Jenny Leigh's Scar, the second culminates in the top of Stokesley Scar, the third and fourth occur in East Scar and the lower part of the fifth forms the uppermost part of the section at Redcar Rocks (Fig. 8). Superimposed on this overall succession there is a long-term, weakly expressed, coarsening upwards trend that is associated with a reduction in parasequence thickness, suggesting that accommodation space was declining. The long-term increase in boring intensity, culminating in the shells found in Stokesley and East Scar, indicates diminishing sedimentation rates and more prolonged exposure on the sea floor compared to shells from the stratigraphically older, and more expanded, Jenny Leigh's Scar shell beds. Brandon et al. (1990) also reported a comparable increase in boring intensity in strata of the Lyra Subchronozone in Lincolnshire.

Similar mud/siltstone-shell bed cycles occur in the Felixkirk borehole, 40km south-west of Redcar (Ivimey-Cook & Powell 1991), and in Lincolnshire, 200 km to the south (Brandon et al. 1990). There, similar cycles continue into higher levels of the Semicostatum Chronozone, as with similar beds reported from the younger succession at Robin Hood's Bay, 40 km south-east of Redcar (Page 2004b). Correlation of individual beds, cycles or parasequences between basins is, however, inconsistent, for example the shell beds of Jenny Leigh's Scar correspond to a mudstone-dominated interval in Lincolnshire, but the Lyra-Scipionianum Subchronozone is characterised by shell beds and siltstones in both regions. Correlation is confounded further by non-sequences in the Bucklandi chronozone in both the Felixkirk Borehole and in Lincolnshire (Brandon et al. 1990; Howard et al. 2009; Ivimey-Cook & Powell 1991)

The mud/siltstone-shell bed cycles represent generally quiet water mudstone deposition interspersed with storm events and subsequent periods of prolonged winnowing, which generated shell beds dominated by the thick-shelled *Cardinia listeri* and *Gryphaea arcuata*. *G. arcuata* is especially common, which led Tate & Blake (1876) to describe these shell beds as 'gryphites'. Shell beds seen at Redcar lack the sharp erosive bases typical of tempestites, and equivalent similar beds in the Felixkirk Borehole show a mixture of sharp and gradational bases. Powell (2010) suggested this was due to mixing of the sediment during post-storm bioturbation. The prolific abundance of *Gryphaea* in the Angulata to Semicostatum chronozones of the British Lower Jurassic may reflect the preservability of their robust shells (Simms 2004; Radley 2008; Pugh et al. 2014), especially so in condensed and winnowed settings.

Interpreted eustatic sea-level curves for UK onshore Lower Jurassic successions are currently based on the Hebrides Basin for the Angulata-Turneri Chronozone interval, combined at higher stratigraphic levels with interpretations from the Cleveland Basin and eventually the Wessex Basin (Hesselbo & Jenkyns 1998; Hesselbo 2008). Relative sea-level change indicated by the Redcar succession is only partially consistent with the Hebridean curve. Thus, a relative sea-level fall indicated during the Rotiforme Subchronozone is coincident with the formation of the Jenny Leigh's Scar shell beds, but relative sea-level rise then purportedly occurs through the Bucklandi Subchronozone to peak in a Lyra Subchronozone highstand (Hesselbo 2008). At Redcar this initial sea-level rise is coincident with the deposition of mudstones (24-32 m, beds 55-64 of Tate & Blake), but other intervals of shallowing within the Bucklandi Subchronozone, not indicated in the Hebrides Basin, saw the formation of the Stokesley Scar shell beds. The Lyra Subchronozone at Redcar records relatively shallow-water deposition in parasequences of diminished thickness compared with the underlying examples. If the relative sea-level rise interpreted in the Hebrides Basin Lyra Subchronozone succession also occurred in the Cleveland Basin, then equivalent parasequences at Redcar would be expected to thicken upwards due to increased accommodation space; quite the opposite is reported in this study. The Redcar succession could instead record a transition from early, aggradation-dominated parasequences to late, progradation-dominated, highstand deposition expressed in a relatively nearshore setting.

The Redcar succession provides insights into the recovery from the end-Triassic mass extinction event. The exact timing of this recovery is contentious as a range of durations for the Hettangian have in recent years been proposed, from earlier

316 estimates of 1.7-2 million years (Schaltegger *et al.* 2008; Ruhl *et al*. 2010; 2016; Guex
317 *et al.* 2012; Hüsing *et al*. 2014) to the most recent cyclostratigraphic estimations of
318 >4.1 million years (Weedon *et al*. 2019). As the Redcar section records the Hettangian-
319 Sinemurian boundary, the age model used has clear implications on the duration of
320 the recovery. Sections elsewhere in the UK have shown that recovery was rapid, with
321 sea floor community structure re-established prior to the Planorbis Chronozone and
322 bivalve diversity essentially stabilising in the mid-Hettangian (Atkinson & Wignall
323 2019). The Redcar section does not expose the lowermost Hettangian, however, it
324 exhibits a faunal assemblage that is diverse and features a wide range of ecological
325 groups seen elsewhere in correlative British Lower Jurassic successions (Brandon *et*
326 *al.* 1990; Atkinson & Wignall 2019). It differs slightly from some other successions in
327 the paucity of large *Plagiostoma giganteum* J. Sowerby and *Pinna similis* Chapuis &
328 Dewalque which abound elsewhere, most notably in the limestone-dominated
329 successions of Glamorgan (Hallam 1960; Atkinson & Wignall 2019; Atkinson *et al.*
330 2019).

331 Bivalve diversity per ammonite zone in the Calcareous Shale Member at
332 Redcar can be compared with recovery trends in the contemporary Scunthorpe
333 Mudstone and Blue Lias formations of the Midlands and southern UK respectively
334 (Table 2). For the Angulata Chronozone the Redcar section appears less diverse than
335 that of the East Midlands Shelf; this may be an effect of more shell beds having been
336 sampled from this zone in the Scunthorpe Mudstone Formation. However, the Redcar
337 succession does host an equivalent bivalve species richness to the contemporaneous
338 Blue Lias of the Dorset Basin.

339 Bucklandi Chronozone bivalve diversity for the Redcar Mudstone Formation
340 exceeds that reported by Brandon *et al*. (1990) for the Scunthorpe Mudstone

Formation and far exceeds the diversity of the Blue Lias in Dorset at this time, but is comparable to the Bristol Channel Basin if additional records from museum collections are included (Atkinson & Wignall 2019). The elevated Redcar diversity may reflect the more habitable conditions of the shallower water Cleveland Basin site, although the prevalence of framboidal pyrite and common occurrences of *Luciniola* suggest the presence of H_2S within the sediment. The entire Redcar succession contains a framboid size distribution suggestive of an oxic-dysoxic water column, again resembling the Bristol Channel Basin of South Wales (Fig.10), and contrasting with evidence of anoxia reported from Central Somerset and Dorset during the Bucklandi Chronozone (Atkinson & Wignall 2019). There are no comparable pyrite framboid studies from the Scunthorpe Mudstone Formation.

Conclusions

Redcar Rocks provide a valuable record of Hettangian/Sinemurian deposition in the Cleveland Basin and allow comparison with the well-documented sections of the Scunthorpe Mudstone Formation of the East Midlands Shelf and the classic Blue Lias of southwest Britain. The Redcar record also allows the current interpretations of sea-level changes during the Hettangian-Sinemurian to be referenced in detail against the Cleveland Basin succession for the first time. The lowest strata belong to the Calcareous Shale Member and are comparable to time-equivalent members of the Scunthorpe Mudstone Formation of the Midlands. Both lack the cyclical development of limestone-marl-shale seen in the Blue Lias Formation. Instead the Calcareous Shale Member features coarsening-upward cycles that grade from mudstones to mass accumulations of *Gryphaea arcuata* and *Cardinia listeri* in sandy shell beds or limestones. Benthic diversity is comparably high through much of the section with a

366 wide range of ecologies represented, suggesting advanced levels of recovery from the
367 end-Triassic mass extinction event some 1.7-4 Myr earlier. Reconstruction of marine
368 oxygenation levels from pyrite framboid populations suggests persistent, though weak,
369 oxygen restriction in the Cleveland Basin and complements the recent findings of
370 Atkinson and Wignall (2019) that showed the majority of the Early Jurassic
371 epicontinental sea in Britain experienced some degree of oxygen restriction.

372

373 **Acknowledgements**

374 We wish to thank the YGS for providing funding for this project via the Yorkshire
375 Geological Society Research Fund in its inaugural year, Tom Charman of Natural
376 England for permissions to sample the Redcar Rocks, Harri Wyn Williams for his
377 excellent thin-section making and Dave Bond for the use of his slide scanner. We also
378 wish to thank John Powell, Mike Simms and Andy Howard (handling editor) for their
379 comments which much improved this work.

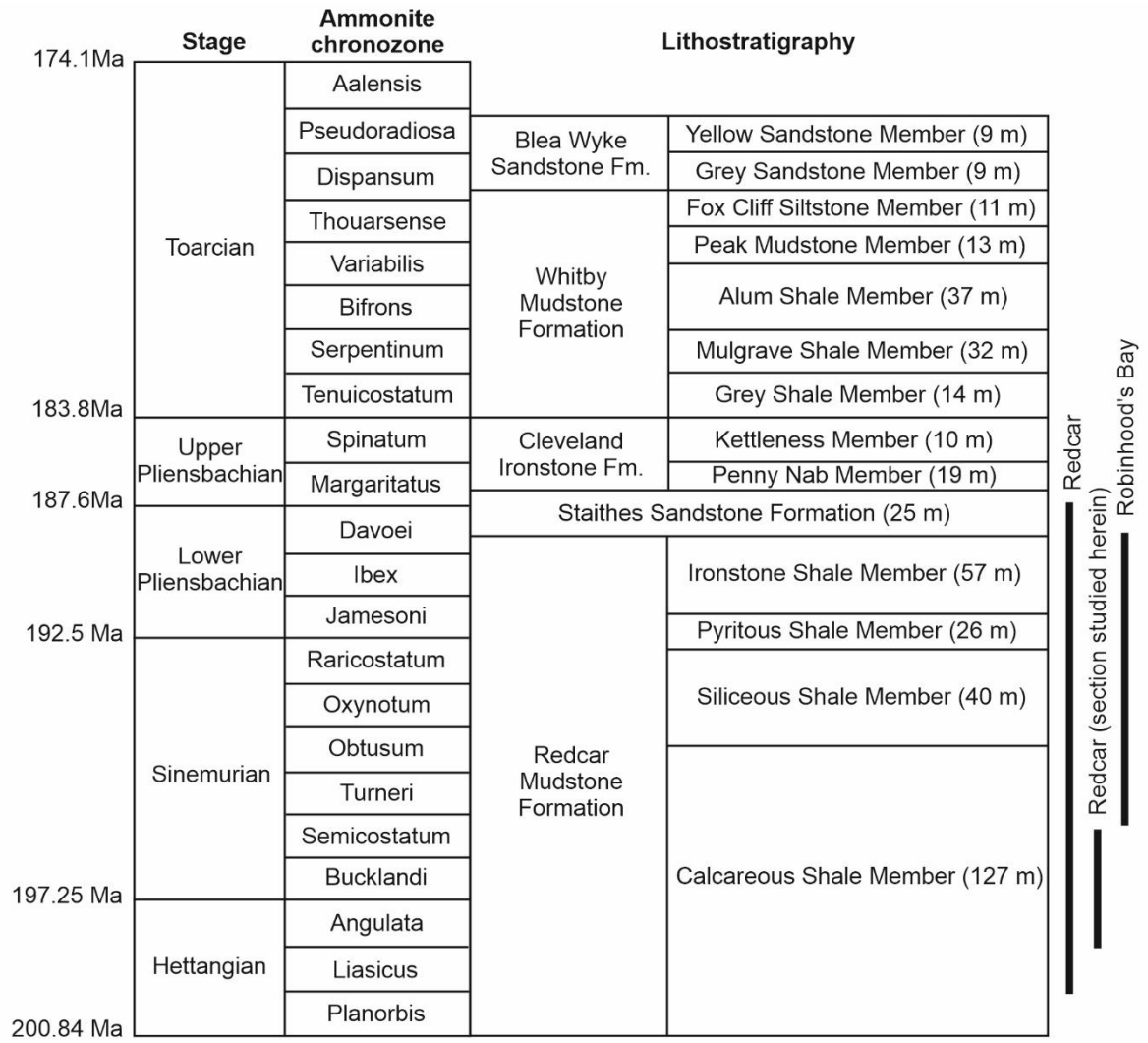

380

381 **Fig. 1** Lithostratigraphical subdivisions and stratigraphical ranges of relevant Lower
382 Jurassic localities in the Cleveland Basin, from Simms (2004). Age model from Ruhl
383 *et al.* (2016) and Weedon *et al.* (2019).

384

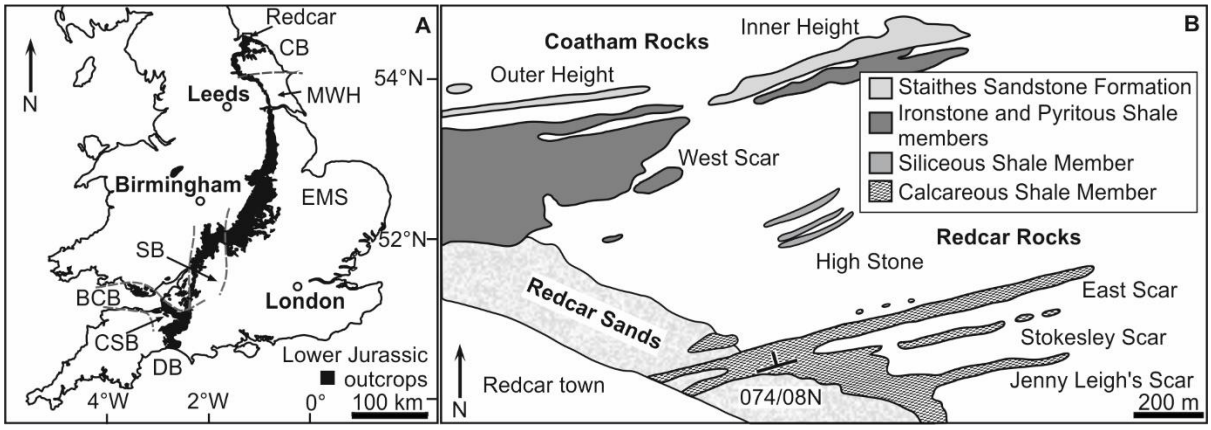

Fig. 2 A. UK location map showing Lower Jurassic outcrop and key sedimentary basins modified from Gründel et al. (2011). Basin codes as follows: DB – Dorset Basin; CSB – Central Somerset Basin; BCB – Bristol Channel Basin; SB – Severn Basin; EMS – East Midlands Shelf; MWH – Market Weighton High; CB – Cleveland Basin. B. Foreshore map of Redcar and Coatham rocks with geological units and scar names (Page 2004a).

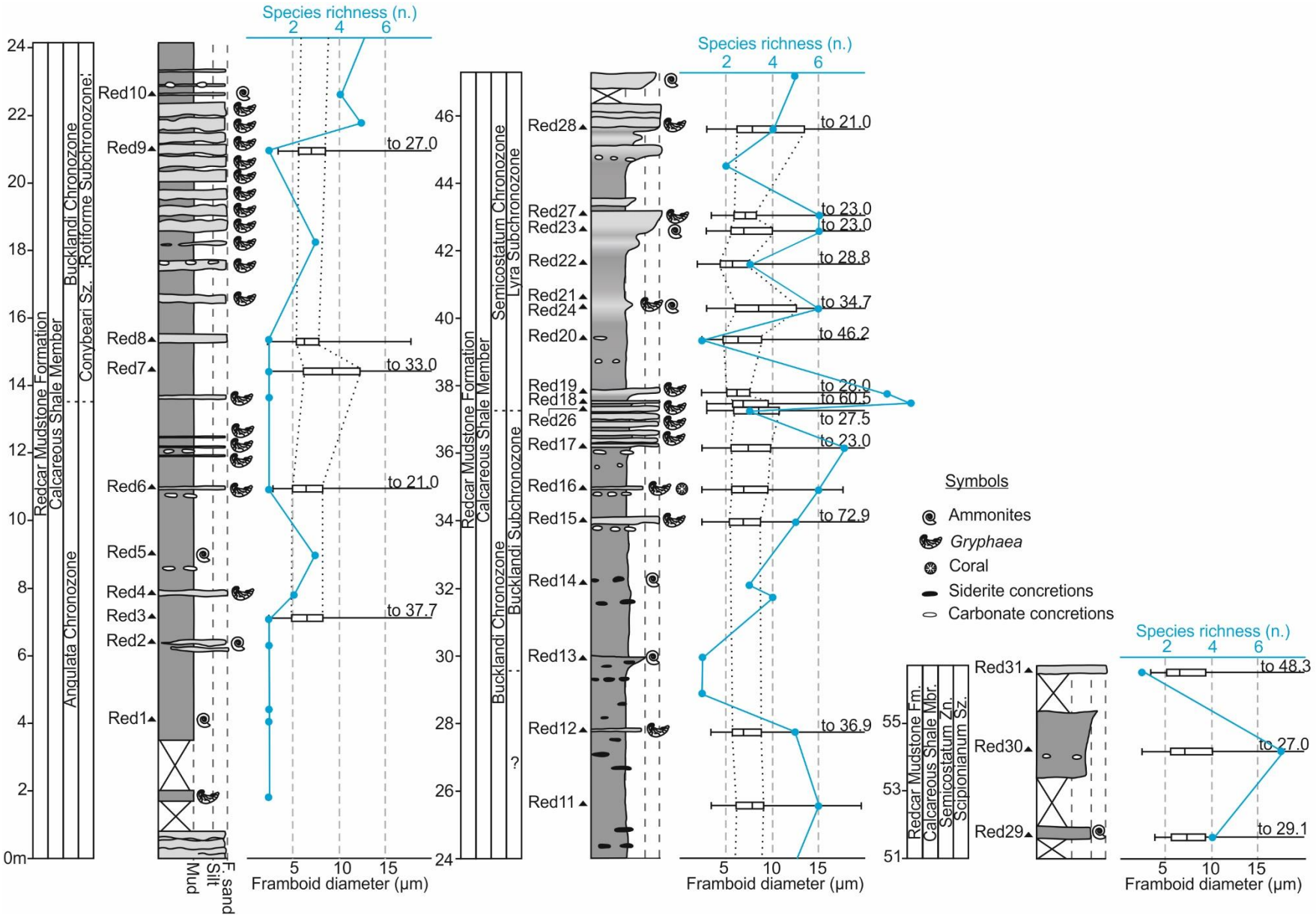
Species richness (n.)
2 4 6
Framboid diameter (μm)
5 10 15
Redcar Mudstone Formation
Calcareous Shale Member
Angulata Chronozone
Bucklandi Chronozone
Conybeari Sz.
Rotiforme Subchronozone
Semicostatum Chronozone
Lyra Subchronozone
Bucklandi Subchronozone
Scipionianum Sz.
Red1
Red2
Red3
Red4
Red5
Red6
Red7
Red8
Red9
Red10
Red11
Red12
Red13
Red14
Red15
Red16
Red17
Red18
Red19
Red20
Red21
Red22
Red23
Red24
Red26
Red27
Red28
Red29
Red30
Red31
to 27.0
to 33.0
to 21.0
to 37.7
to 21.0
to 23.0
to 23.0
to 28.8
to 34.7
to 46.2
to 28.0
to 60.5
to 27.5
to 23.0
to 72.9
to 36.9
to 48.3
to 27.0
to 29.1
Mud
Silt
F. sand
Symbols
Ammonites
Gryphaea
Coral
Siderite concretions
Carbonate concretions

Fig. 3 Graphic log of Redcar Rocks including box and whisker plots of pyrite framboid analyses. Each box depicts 25th and 75th percentiles, central line is median, whiskers illustrate minimum and maximum framboid diameters. Solid circles show raw species richness per sampled horizon.

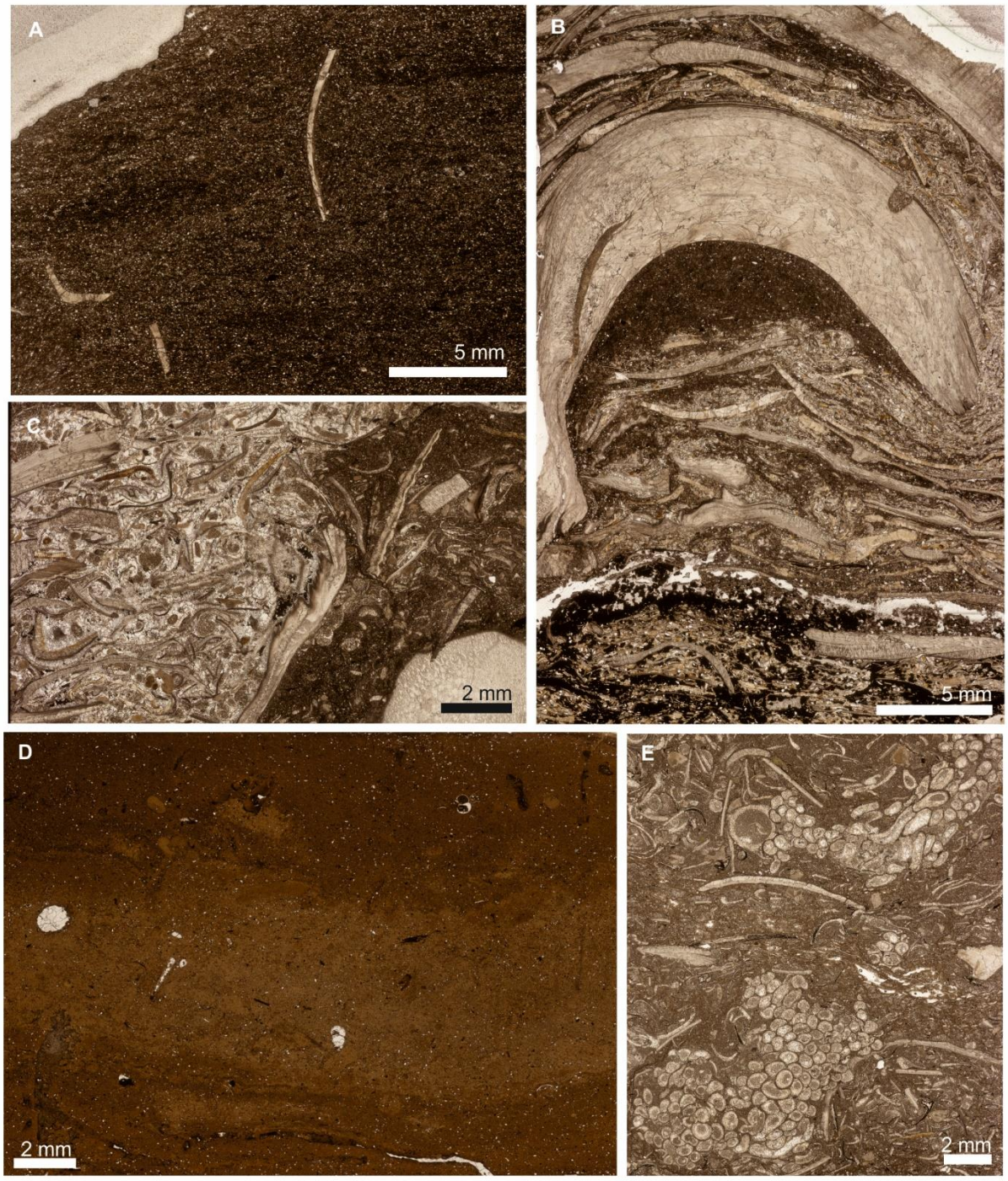

Fig. 4 Photomicrographs of thin sections. A. Red 23, Mudstone with shell fragment rotated by burrowing. B. Red 28, example shell bed including *Gryphaea* shell with simple boring on the right. C. Red 6, example of biosparite D. Red 24, phosphatic nodule featuring burrow mottling. E. Red 8, two nests of serpulid tubes.

Fig. 5 *Gryphaea*-rich shell bed (Red 19) at outcrop. Hammer 30 cm long.

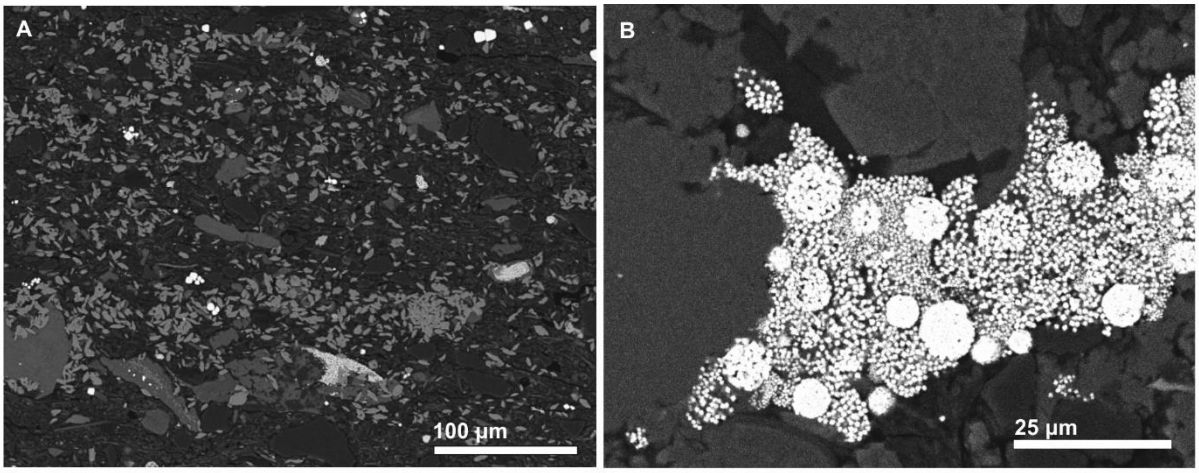

Fig. 6 SEM images. A. Red 11, silty mudstone with abundant ankerite grains, appearing as pale grey, rice-shaped grains in cross section. B. Red 15, shell bed limestone with pyrite framboids surrounded by a cloud of dissociated pyrite microcrysts.

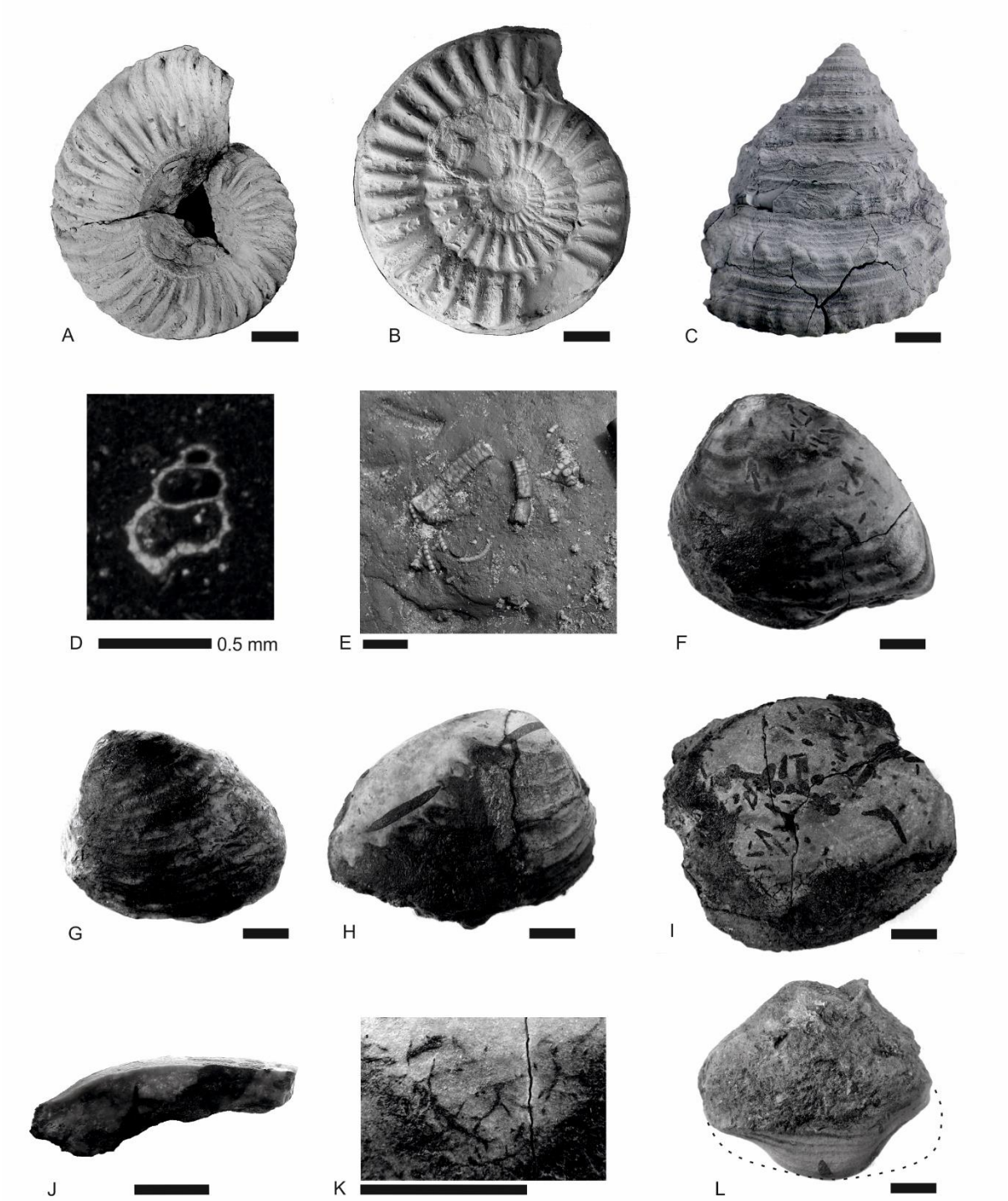

411

412 **Fig. 7** Examples of fossils collected from Redcar; specimens housed in Whitby
413 Museum. A. Red 1, *Schlothemia* sp. (WHITM: 2020/1.1); B. Red 21, *Arnioceras* sp.
414 encrusted by *Liostrea irregularis* (Münster) (WHITM 2020/1.2); C. Red 17,
415 *Pleurotomaria cognata* Chapuis & Dewalque (WHITM: 2020/1.3); D. Red 2
416 photomicrograph of microgastropod in thin section; E. Red 12 *Isocrinus psilonoti*

(Quenstedt), partially articulated specimen with cirri, photographed *in situ;* F – I. Red 15, *Cardinia listeri* (J. Sowerby) featuring a range of cirripede borings (WHITM: 2020/1.4-8). J. cross-section through part of *C. listeri* shell (I) showing potential *Simonizapfes*; K. detail of *C. listeri* shell (I) with possible bryozoan borings; L. *C. listeri* with growth defect, dashed line projects normal shell outline. A-C whitened using ammonium chloride, scale bars 1 cm unless otherwise stated.

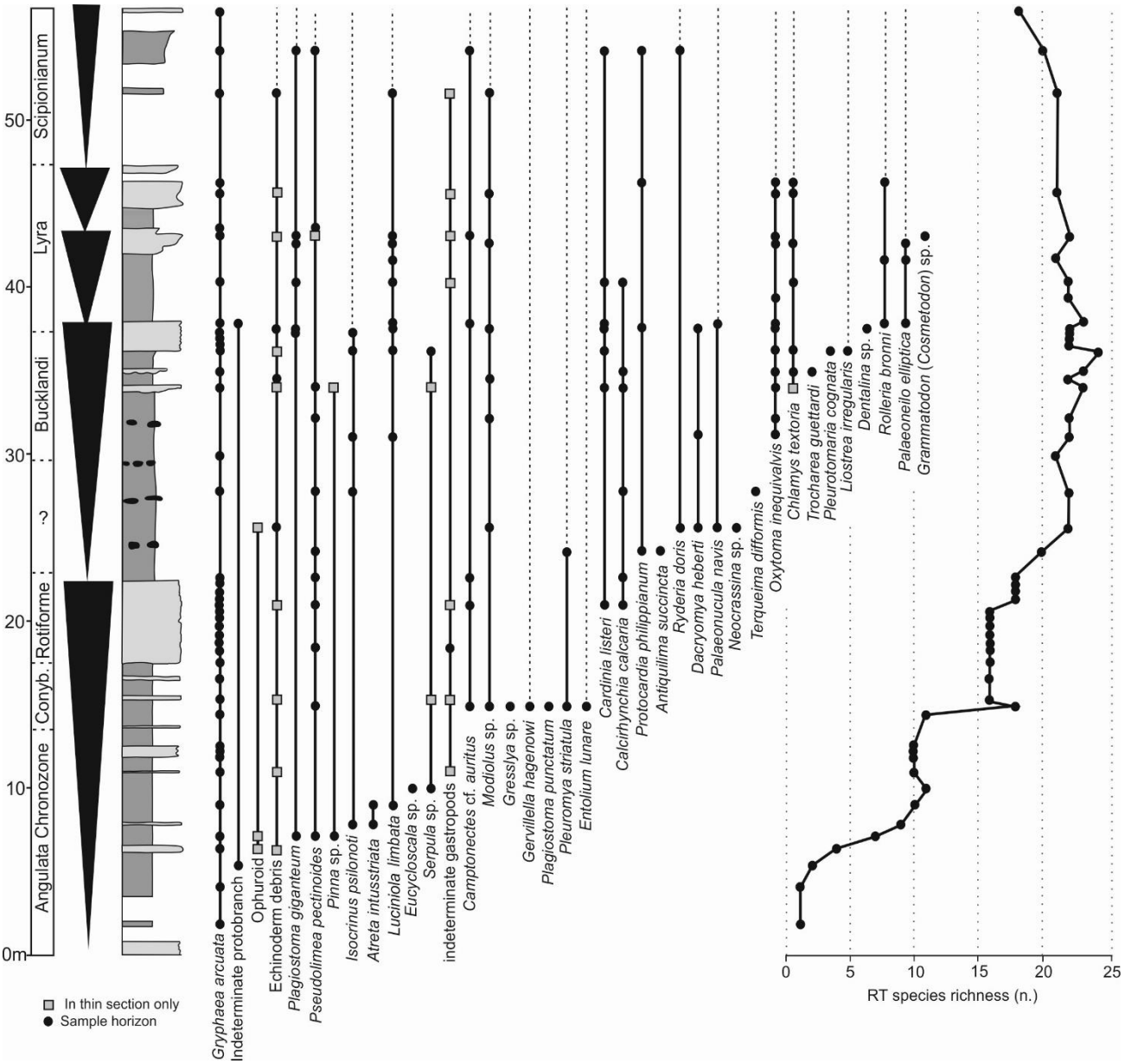

Fig. 8 Species range chart and Range Through (RT) species richness for Redcar Rocks. For range chart, dark circles show horizons that species were encountered

during field collections, shaded squares for species encountered only in thin sections. Connecting line indicates range of species, extensions to ranges based on personal observations and species occurrence data presented in Atkinson and Wignall (2020). Inverted black triangles on the left indicate the stratigraphic range of the five parasequences.

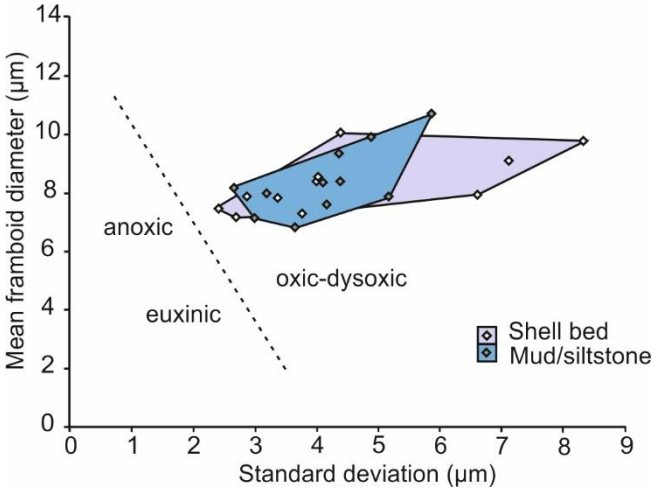

Fig. 9 Mean framboid diameter (µm) against standard deviation of framboid diameters (Wilkin diagram) for Redcar. Dashed line indicates anoxic/oxic-dysoxic threshold (Wilkin *et al.* 1996). Samples plotted as being either from shell beds or from the intervening mudstones and siltstones, with shaded regions illustrating the spread of results.

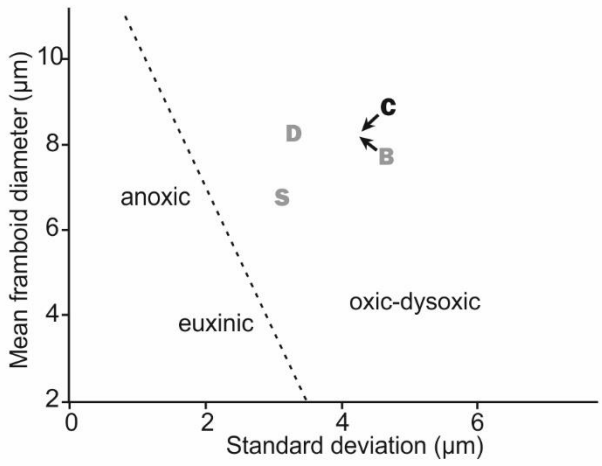

438 **Fig. 10** Average framboid diameter and standard deviation for the Blue Lias in three
439 basins in southwest Britain. D – Dorset Basin; B – Bristol Channel Basin; S – Central
440 Somerset Basin (from Atkinson & Wignall 2019); C – Cleveland Basin (this study).

441

442

SPECIES	***ECOLOGY***
Gryphaea arcuate Lamarck	surficial, non-motile, reclining suspension feeder
Atreta intusstriata (Emmrich)	surficial, cemented, suspension feeder
Terquemia difformis (Schlotheim)	surficial, cemented, suspension feeder
Liostrea irregularis (Münster)	surficial, cemented, suspension feeder
Plagiostoma giganteum J. Sowerby	epibyssate, suspension feeder
Plagiostoma punctatum J. Sowerby	epibyssate, suspension feeder
Pseudolimea pectinoides (J. Sowerby)	epibyssate, suspension feeder
Antiquilima succincta (Schlotheim)	epibyssate, suspension feeder
Grammatodon (Cosmetodon) sp.	epibyssate, suspension feeder
Oxytoma inequivalvis (J. Sowerby)	epibyssate, suspension feeder
Camptonectes cf.auritus (Schlotheim)	epibyssate, suspension feeder
Chlamys textoria (Schlotheim)	epibyssate, suspension feeder
Entolium lunare (Roemer)	surficial, facultative motile, suspension feeder
Modiolus sp.	endobyssate, suspension feeder
Pinna sp.	endobyssate, suspension feeder
Cuneigervillia hagenowi (Dunker)	endobyssate, suspension feeder
Neocrassina sp.	shallow infaunal, suspension feeder
Cardinia listeria (J. Sowerby)	shallow infaunal, suspension feeder
Protocardia philippianum (Dunker)	shallow infaunal, suspension feeder
Luciniola limbata (Terquem & Piette)	shallow infaunal, suspension feeder with chemosymbionts
Dacryomya heberti (Martin)	shallow infaunal, deposit feeder
Palaeonucula navis (Piette)	shallow infaunal, deposit feeder
Ryderia doris (d'Orbigny)	shallow infaunal, deposit feeder
Rollieria bronni (Andler)	shallow infaunal, deposit feeder
Palaeoneilo elliptica (Goldfuss)	shallow infaunal, deposit feeder
indeterminate protobranch	shallow infaunal, deposit feeder
Gresslya sp.	deep infaunal, suspension feeder
Pleuromya striatula Agassiz	deep infaunal, suspension feeder

443 **Table 1** Bivalve ecologies encountered within the Redcar sequence, assigned from
444 published literature (Johnson 1984; Hodges 1991, 2018; Wignall 1990; Damborenea
445 & Manceñido 2005; Ros-Franch *et al.* 2014)

BASIN	***ANGULATA***	***BUCKLANDI***	***SEMICOSTATUM***
Cleveland	7	23 (24)	16 (20)
East Midlands Shelf	14	8 (13)	29 (30)
Dorset	8	Under sampled	6
Central Somerset	11	12	Nd.
Bristol Channel	17 (28)	13 (26)	29
Severn	Nd.	13	Nd.

446

447 **Table 2** Bivalve species richness per chronozone for four basins of the classic Blue
448 Lias Formation and the Scunthorpe Mudstone Formation from the East Midlands Shelf
449 compared with the correlative succession in the Cleveland Basin. Bracketed values
450 show Range Through bivalve species richness, for Bristol Channel Basin this value
451 includes specimens housed in the National Museum of Wales. Bivalve species
452 richness data from Atkinson and Wignall (2019; 2020) and Brandon et al. (1990).

453

454 References

455 Atkinson, J.W. & Wignall, P.B. 2019. How quick was marine recovery after the end-
456 Triassic mass extinction and what role did anoxia play? *Palaeogeography,*
457 *Palaeoclimatology, Palaeoecology*, **528**, 99–119,
458 https://doi.org/10.1016/j.palaeo.2019.05.011.

459 Atkinson, J.W & Wignall, P.B. 2020. Body size trends and recovery amongst bivalves
460 following the end-Triassic mass extinction. *Palaeogeography, Palaeoclimatology,*
461 *Palaeoecology*, **538**, https://doi.org/10.1016/j.palaeo.2019.109453

462 Atkinson, J.W., Wignall, P.B., Morton, J.D. & Aze, T. 2019. Body size changes in
463 bivalves of the family Limidae in the aftermath of the end-Triassic mass extinction:
464 the Brobdingnag effect. *Palaeontology*, **62**, 561-582,
465 https://doi.org/10.1111/pala.12415.

466 Brandon, A., Slumber, M.G. & Ivimey-Cook, H.C. 1990. A revised lithostratigraphy for
467 the Lower and Middle Lias (Lower Jurassic) east of Nottingham, England.
468 *Proceedings of the Yorkshire Geolocial Society*, **48**, 121-141,
469 https://doi.org/10.1144/pygs.48.2.121

470 Cohen, A.S., Coe, A.L., Harding, S.M. & Schwark, L. 2004. Osmium isotope evidence
471 for the regulation of atmospheric CO_2 by continental weathering. *Geology,* **32**,
472 157-160, https://doi.org/10.1130/G20158:1

473 Damborenea, S. & Manceñido, M.O. 2005. Biofacies analysis of Hettangian-
474 Sinemurian bivalve/brachiopod associations from the Neuquén Basin (Argentina).
475 *Geologica Acta*, **3**, 163–178, https://doi.org/10.1344/105.000001405.

476 Danise, S., Twitchett, R.J., Little, C.T.S. & Clémence, M.-E. 2013. The impact of global
477 warming and anoxia on marine benthic community dynamics : an example from
478 the Toarcian (Early Jurassic). *PLoS ONE*, **8**, e56255,
479 https://doi.org/10.1371/journal.pone.0056255.

480 Gad, M.A.M.A. 1966. *A Geochemical Study of the Liassic Rocks of the Yorkshire*
481 *Coast*. University of London.

482 Gründel, J., Kaim, A., Nützel, A. & Little, C.T.S. 2011. Early Jurassic gastropods from

England. *Palaeontology*, **54**, 481–510, https://doi.org/10.1111/j.1475-4983.2011.01043.x.

Guex, J., Schoene, B. *et al.* 2012. Geochronological constraints on post-extinction recovery of the ammonoids and carbon cycle perturbations during the Early Jurassic. *Palaeogeography Palaeoclimatology Palaeoecology*, **346–347**, 1–11. https://doi.org/10.1016/j.palaeo.2012.04.030.

Hallam, A. 1960. A sedimentary and faunal study of the Blue Lias of Dorset and Glamorgan. *Philosophical Transactions of the Royal Society of London B: Biological Sciences*, **243**, 1–44, https://doi.org/10.1098/rstb.1960.0003.

Häntzschel, W. 1975. *Treatise on Invertebrate Paleontology Part W Miscellanea Supliment 1. Trace Fossils and Problematica*, 2nd ed. Teichert, C. (ed.). Boulder, The Geological Society of America, Inc. and The Universtiy of Kansas.

Hesselbo, S.P. 2008. Sequence stratigraphy and inferred relative sea-level change from the onshore British Jurassic. *Proceedings of the Geologists' Association*, **119**, 19–34, https://doi.org/10.1016/S0016-7878(59)80069-9.

Hesselbo, S.P. & Jenkyns, H.C. 1998. British Lower Jurassic sequence stratigraphy. *In*: *Mesozoic and Cenozoic Sequence Stratigraphy of European Basins*. SEPM Special Publications No. 60.

Hodges, P. 1991. The relationship of the Mesozoic bivalve *Atreta* to the Dimyidae. *Palaeontology*, **34**, 963–970.

Hodges, P. 2018. *The Early Jurassic Bivalvia from the Hettangian and Lower Sinemurian of South-West Britain Part 2*. London, Monograph of the Palaeontographical Society, https://doi.org/10.1080/02693445.2017.11963960.

Howard, A.S., Warrington, G. et al. 2009. Geology of the Nottingham district. *Memoir*

of the British Geological Survey, Sheet 126 (England and Wales)

Hüsing, S.K., Beniest, A. et al. 2014. Astronomically-calibrated magnetostratigraphy of the LowerJurassic marine successions at St. Audrie's Bay and East Quantoxhead (Hettangian-Sinemurian; Somerset, UK). *Palaeogeography*,*Palaeoclimatology, Palaeoecology*, **403**, 43–56. https://doi.org/10.1016/j.palaeo.2014.03.022

Ivimey-Cook, H.C. & Powell, J.H. 1991. Late Triassic and early Jurassic biostratigraphy of the Felixkirk Borehole, North Yorkshire. *Proceedings of the Yorkshire Geological Society*, **48**, 367–374.

Johnson, A. 1984. *The Palaeobiology of the Bivalve Families Pectinidae and Propeamussiidae in the Jurassic of Europe*. München, Zitteliana.

Kemp, D.B, Coe, A.L., Cohen, A.S. & Schwark, L. 2005. Astronomical pacing of methane release in the Early Jurassic period. *Nature,* **437**, 396-399, https://doi.org/10.1038/nature03983

Little, C.T.S. & Benton, M.J. 1995. Early Jurassic mass extinction : A global long-term event. *Geology*, **23**, 495–498, https://doi.org/10.1130/0091-7613(1995)023<0495.

Lord, A. 1971. Revision of some Lower Lias ostracoda from Yorkshire. *Palaeontology*, **14**, 642-665.

McArthur, J.M., Donovan, D.T., Thirlwall, M.F., Fouke, B.W & Mattey, D. 2000. Strontium isotope profile of the early Toarcian (Jurassic) ocean anoxic event, the duration of ammonite biozones, and belemnite palaeotemperatures. *Earth and Planetary Science Letters,* **179**, 269-285, https://doi.org/10.1016/S0012-821X(00)00111-4

Meister, C., Aberhan, M., et al. 2004. The Global Boundary Stratotype Section and Point (GSSP) for the base of the Pliensbachian Stage (ower Jurassic), Wine Haven , Yorkshire , UK. *Episodes*, **29**, 93–106.

Negus, P.E. 1983. Distribution of the British Jurassic corals. *Proceedings of the Geologists' Association*, **94**, 251–257, https://doi.org/10.1016/S0016-7878(83)80043-1.

Page, K.N. 1992. The sequence of ammonite correlated horizons in the British Sinemurian (Lower Jurassic). *Newsletters in Stratigraphy* **27**, 129-156.

Page, K.N. 2010b. Stratigraphical Framework. In: Lord, A.R. and Davis, P.G. Fossils from the Lower Lias of the Dorset Coast, Palaeontological Association Field Guide to Fossils 13: 33-53.

Page, K.N. 2004a. Redcar Rocks. *In*: Simms, M. J., Chidlaw, N., Morton, N. & Page, K. N. (eds) *British Lower Jurassic Stratigraphy*. Peterborough, Geological Conservation Review Series, No. 30, Joint Nature Conservation committee, 245–250.

Page, K.N. 2004b. Normanby Stye Batts-Miller's Nab (Robin Hood's Bay). *In*: Simms, M. J., Chidlaw, N., Morton, N. & Page, K. N. (eds) *British Lower Jurassic Stratigraphy*. Peterborough, Geological Conservation Review Series, No. 30, Joint Nature Conservation committee, 250–262.

Patacci, M. 2016. A high-precision Jacob's staff with improved spatial accuracy and laser sighting capability. *Sedimentary Geology*, **335**, 66–69, https://doi.org/DOI: 10.1016/j.sedgeo.2016.02.001.

Powell, J.H. 1984. Lithostratigraphical nomenclature of the Lias Group in the Yorkshire Basin. *Proceedings of the Yorkshire Geological Society*, **45**, 51–57.

555 Powell, J.H. 2010. Jurassic sedimentation in the Cleveland Basin : a review.
556 *Proceedings of the Yorkshire Geological Society*, **58**, 21–72,
557 https://doi.org/10.1144/pygs.58.1.278.

558 Powell, J.H., Cooper, A.C. & Benfield, A.C. 1992. *Geology of the County around*
559 *Thirsk*. British Geological Survey Memoir, England and Wales, Sheet 52.

560 Pugh, A.C., Danise, S., Brown, J.R. & Twitchett, R.J. 2014. Benthic ecosystem
561 dynamics following the Late Triassic mass extinction event : Palaeoecology of the
562 Blue Lias Formation, Lyme Regis, UK. *Proceedings of the Ussher Society*, **13**,
563 255–266.

564 Radley, J.D. 2008. Gryphaea beds (upper Scunthorpe Mudstone Formation; Lower
565 Jurassic) at Scunthorpe, North Lincolnshire, north-east England. *Proceedings of*
566 *the Yorkshire Geological Society*, **57**, 107–111.

567 Rita, P., Reolid, M. & Duarte, L. V. 2016. Benthic foraminiferal assemblages record
568 major environmental perturbations during the Late Pliensbachian – Early Toarcian
569 interval in the Peniche GSSP, Portugal. *Palaeogeography, Palaeoclimatology,*
570 *Palaeoecology*, **454**, 267–281, https://doi.org/10.1016/j.palaeo.2016.04.039.

571 Ros-Franch, S., Márquez-aliaga, A. & Damborenea, S.E. 2014. Comprehensive
572 database on Induan (Lower Triassic) to Sinemurian (Lower Jurassic) marine
573 bivalve genera and their paleobiogeographic record. *Paleontological*
574 *Contributions*, **8**, 1–219, https://doi.org/10.17161/PC.1808.13433.

575 Ruhl, M., Deenen, M.H.L., Abels, H.A., Bonis, N.R., Krijgsman, W. & Kürschner, W.M.
576 2010. Astronomical constraints on the duration of the early Jurassic Hettangian
577 stage and recovery rates following the end-Triassic mass extinction (St Audrie's
578 Bay / East Quantoxhead, UK). *Earth and Planetary Science Letters*. **295**, 262–

276. https://doi.org/10.1016/j.epsl.2010.04.008.

Ruhl, M., Hesselbo, S.P. *et al.* 2016. Astronomical constraints on the duration of the Early Jurassic Pliensbachian Stage and global climate fluctuations. *Earth and Planetary Science Letters,* **455**, 149-165, https//doi.org/10.1016/j.epsl.2016.08.038

Schaltegger, U., Guex, J., Bartolini, A., Schoene, B. & Ovtcharova, M. 2008. Precise U–Pb age constraints for end-Triassic mass extinction, its correlation to volcanism and Hettangian post-extinction recovery. *Earth and Planetary Science Letters,* **267**, 266–275. https://doi.org/10.1016/j.epsl.2007.11.031.

Simms, M.J. 2004. Hock Cliff. *In*: Simms, M. J., Chidlaw, N., Morton, N. & Page, K. N. (eds) *British Lower Jurassic Stratigraphy*. Peterborough, Geological Conservation Review Series, No. 30, Joint Nature Conservation committee, 164–170.

Simms, M.J. 2004. The Cleveland Basin, Introduction. *In*: Simms, M. J., Chidlaw, N., Morton, N. & Page, K. N. (eds) *British Lower Jurassic Stratigraphy*. Peterborough, Geological Conservation Review Series, No. 30, Joint Nature Conservation committee, 239–245.

Tate, R. & Blake, J.F. 1876. *The Yorkshire Lias*. London.

Trueman, A.E. 1930. The lower Lias (bucklandi Zone) of Nash Point, Glamorgan. *Proceedings of the Geologists' Association*, **41**, 148–159.

van Buchem, F.S.P. & McCave, I.N. 1989. Cyclic sedimentation patterns in Lower Lias mudstones of Yorkshire (GB). *Terra Nova*, **1**, 461–467.

Weedon, G.P., Page, K.N. & Jenkyns, H.C. 2019. Cyclostratigraphy, stratigraphic gaps and the duration of the Hettangian Stage (Jurassic): insights from the Blue Lias Formation of southern Britain. *Geological Magazine*, **156,** 1469–1509,

https://doi.org/10.1017/S0016756818000808.

Wignall, P.B. 1990. Benthic palaeocology of the Late Jurassic Kimmeridge Clay of England. *Special papers in palaeontology*, **43**.

Wignall, P.B. & Newton, R.J. 1998. Pyrite framboid diameter as a measure of oxygen deficiency in ancient mudrocks. *Americna Journal of Science*, **298**, 537–552, https://doi.org/10.2475/ajs.298.7.537.

Wignall, P.B., Newton, R.J. & Little, C.T.S. 2005. The timing of paleoenvironmental change and cause-and-effect relationships during the Early Jurassic mass extinction in Europe. *American Midland Naturalist*, **305**, 1014–1032.

Wilkin, R.T., Barnes, H.L. & Brantley, S.L. 1996. The size distribution of framboidal pyrite in modern sediments: An indicator of redox conditions. *Geochimica et Cosmochimica Acta*, **60**, 3897–3912, https://doi.org/10.1016/0016-7037(96)00209-8.